Estimation of the Cutting Torque Without a Speed Sensor During CNC Turning

Won Tae Kwon*
Department of Mechanical and Information Engineering, University of Seoul, 90 Cheonnong-dong Tongdaemun-gu, Seoul 130-743, Korea
Ik jun Hong
Department of Mechanical and Information Engineering, University of Seoul, 90 Cheonnong-dong Tongdaemun-gu, Seoul 130-743, Korea

In this paper, the cutting torque of a CNC machine tool during machining is monitored through the internet. To estimate the cutting torque precisely, the spindle driving system is divided into two parts: electrical induction motor part and mechanical part. A magnetized current is calculated from the measured three-phase stator currents and used for the total torque estimation generated by a spindle motor. Slip angular velocity is calculated from the magnetized current directly, which gets rid of the necessity of a spindle speed sensor. Since the frictional torque changes according to the cutting torque and the spindle rotational speed, an experiment is adopted to obtain the frictional torque as a function of the cutting torque and the spindle rotation speed. Then the cutting torque can be calculated by solving a 2^{nd} order difference equation at a given cutting condition. A graphical programming method is used to implement the torque monitoring system developed in this study to the computer and at the same time monitor the torque of the spindle motor in real time through the internet. The cutting torque of the CNC lathe is estimated well within an about 3% error range in average in various cutting conditions.

Key Words: Internet Torque Monitoring, Magnetized Spindle Motor Current, Mechanical Friction

Nomenclature

B : Equivalent damping ratio [Nm]
i_{ds}, i_{qs} : Stator current in d, q direction [A]
i_{mr} : Magnetized current [A]
J : Equivalent inertia applied to the motor axis [Nm^2]
L_m : Mutual inductance between stator and rotor [H]
L_r : Inductance of rotor [H]
p : Number of poles
R_r : Resistance of rotor [Ω]
T_c : Cutting torque [Nm]
T_e : Electrically generated torque from the spindle motor [Nm]
T_{fco} : Coulomb frictional force with no load
T_t : Total torque applied to the motor [Nm]
δT_f : Increment of the frictional torque due to cutting torque increment
δT_{fc} : Increment of the Coulomb frictional torque increment due to cutting torque increment
δT_{fv} : Increment of the damping torque due to cutting torque increment
$\lambda_{dr}, \lambda_{qr}$: Magnetic flux of rotor in d, q direction
λ_r : Magnetic flux of rotor
$\omega, \omega_r, \omega_{sl}$: Synchronized, rotor and slip angular velocity of the spindle motor [rad/sec.]

* Corresponding Author,
E-mail : kwon@uos.ac.kr
TEL : +82-2-2210-2403; **FAX** : +82-2-2248-5110
Department of Mechanical and Information Engineering, University of Seoul, 90 Cheonnong-dong Tongdaemun-gu, Seoul 130-743, Korea. (Manuscript **Received** March 31, 2005; **Revised** October 28, 2005)

1. Introduction

Cutting force is well known to be one of the best signals to monitor a cutting condition. Among various cutting force measuring equipments, a tool dynamometer has been the most widely used for the cutting force measurement in a laboratory owing to its accuracy and wide bandwidth of the measured signal. However, drawbacks such as high price, installation difficulty, limitation of a workpiece size, electrical wiring problem and restriction of using cutting fluid, have been preventing it from being used in an industrial environment. To overcome these difficulties, a variety of indirect cutting force measurement systems have been developed over the years. Huh estimated the cutting force using the RMS value of three-phase currents, total power and the modeling of the spindle driving system on the CNC lathe (Lee et al., 1998 ; Huh et al., 1999). Stein and Wang proposed a cutting force estimation method using the current of the DC feed motor (Stein et al., 1986). Choi monitored the average cutting torque using the average spindle motor power per revolution during the milling process (Choi, 1997), and Park and Luca presented a linear model to estimate the cutting torque during the drilling process (Park and Luca, 1994). Mannan monitored the cutting process using the power and the current of both spindle and feed direction motors (Mannan and Broms, 1989). Since the measurement of the total power in the spindle system is relatively easy and needs no speed measurement sensor, it has become one of the most widely used technologies for the estimation of the cutting torque. However, motor power includes not only the power used to overcome the cutting torque and the power dissipated in stator and rotor circuits, but also the power fluctuation due to internal inductance and the torque consumed to overcome frictional force in the mechanical system.

In this study, the spindle driving system was divided into two parts for the analysis, electrical induction motor part and mechanical part. We measured the stator currents, from which the magnetized current was derived to determine the angular velocity of the spindle motor. We also calculated the magnetic flux and the generated torque from the spindle motor using both stator and magnetized currents. The procedure of estimating the spindle motor velocity removed the necessity of an encoder. In the mechanical part, frictional torque was formulated as a function of angular velocity and cutting torque and consequently determined the cutting torque more precisely. A graphical programming method was used to implement the torque monitoring system to the computer and to monitor the torque of a spindle motor in real time through the internet.

2. Estimation of the Angular Velocity and Torque of an Induction Motor

2.1 Estimation of the generated torque without a speed sensor

D-q voltage equation of an induction motor in the synchronized rotating coordinate is given in Eqs. (1) and (2) (Chung, 1993).

$$\lambda_{dr}=L_r i_{dr}+L_m i_{ds}=L_m i_{dr} \tag{1}$$

$$\lambda_{qr}=L_r i_{qr}+L_m i_{qs} \tag{2}$$

When the reference frame is fixed in the rotor, the magnetic flux of the rotor in q direction (λ_{qr}) was 0, and the magnetic flux of the rotor in d direction (λ_{dr}) is constant. In this case, a first order ordinary differential equation to calculate the magnetized current from the measured stator current can be obtained as follows (Chung, 1993),

$$i_{mr}+\left(\frac{L_r}{R_r}\right)\frac{di_{mr}}{dt}=i_{ds} \tag{3}$$

The slip angular velocity can be also obtained as follows.

$$\omega_{sl}=\frac{R_r\left(-\frac{L_m}{L_r}\right)i_{qs}}{L_m i_{mr}}=\frac{i_{qs}}{\left(\frac{L_r}{R_r}\right)i_{mr}} \tag{4}$$

After the slip angular velocity was obtained, the angular velocity of the motor is easily calculated from the fact that the slip angular velocity is the difference between the synchronized angular velocity and the spindle angular velocity. The synchronized angular velocity is the angular velocity of the stator current.

$$\omega_r=\omega-\omega_{sl}=\omega-\frac{i_{qs}}{\left(\frac{L_r}{R_r}\right)i_{mr}}=\omega-\frac{L_m i_{qs}}{\left(\frac{L_r}{R_r}\right)\lambda_r} \quad (5)$$

where $\lambda_r=L_m i_{mr}$

The torque generated by the spindle induction motor is as follows.

$$T_e=\frac{3}{2}\frac{p}{2}\frac{L_m}{L_r}\lambda_r i_{qs} \quad (6)$$

Consequently, the electrically induced torque in the induction motor can be calculated by the Eq. (6), in which the i_{qs} is measured and the λ_r is obtained from the equation $\lambda_r=L_m i_{mr}$, while parameters p, L_m, L_r are given.

2.2 Modeling of the mechanical part of the spindle system

The mechanical part of the spindle motor system which includes a motor axis, a gear box and a spindle head can be expressed by the first order differential equation of the angular velocity as in Eq. (7).

$$J\frac{d\omega_r}{dt}+B\omega_r=T_e-T_t \quad (7)$$

In the Eq. (7), T_t is the total equivalent torque applied to the motor and is the sum of the frictional, damping, and cutting torques (Lee et al., 1998).

$$\begin{aligned}T_t&=T_{fc0}+\delta T_f+T_c\\&=T_{fc0}+\delta T_{fc}+\delta T_{fv}+T_c\end{aligned} \quad (8)$$

Here, δT_f is the increment of the frictional force due to the increase in cutting force and is composed of two components, δT_{fc} and δT_{fv}. Hence, it is necessary to find the relationship between δT_{fc}, δT_{fv} and the cutting torque, T_c to determine the relationship between δT_f and T_c. T_{fco} is the experimentally obtained Coulomb frictional torque with no load.

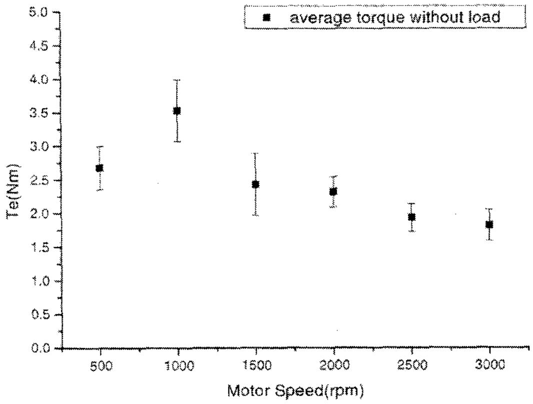

Fig. 1 Average torque without load according to motor speed variation

In the steady state, the angular velocity is kept constant ($d\omega_r/dt=0$). Since δT_f and T_c are 0 during idling, the Eq. (7) becomes,

$$B\omega_r=T_e-T_{fc0} \quad (9)$$

Eq. (9) could be rewritten as,

$$T_e=B\omega_r+T_{fc0} \quad (10)$$

In the Eq. (10), T_e was expressed as a linear function of ω_r. As a result of an experimental measurement of T_e and ω_r, constants B and T_{fc0} can be obtained from the experimental data. T_e at various speeds was measured to determine the B and T_{fc0}, and the results are given in Fig. 1. The parabola seems to be the best fit for the measurements. However, two linear equations are used to fit the data instead of the parabola, due to the linear relationship between T_e and ω_r as given in Eq. (10), and we obtained the values of B and T_{fc0} at below and above 1000 rpm, respectively.

To figure out the effect of the running time of the CNC machine on B and T_{fc0}, some experiments were carried out during an extended time. After the CNC machine was turned on, the spindle kept on running without load for 6 hours, and T_es were measured for every 30 minutes. Experiments were executed at different cutting velocities from 500 to 3000 rpm under the condition of 24.5℃ ~27.2 ℃ and 35~46% relative humidity. The results are given in Figs. 2 and 3. As

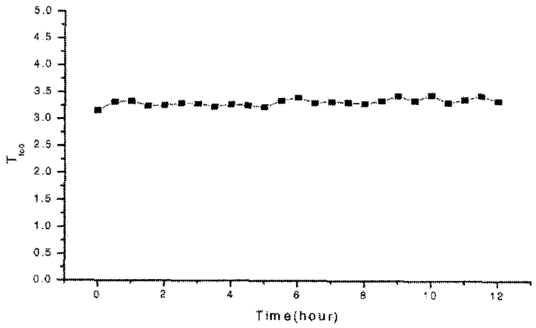

Fig. 2 Coulomb friction variation according to time (above 1000 rpm)

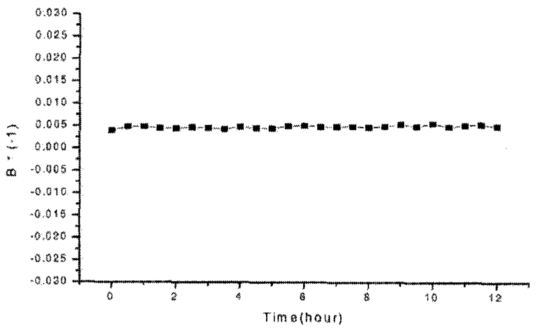

Fig. 3 Damping coefficient variation according to time (above1000 rpm)

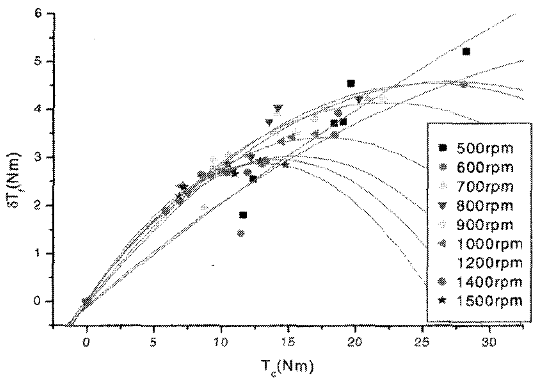

Fig. 4 Nonlinear friction torque during machining

shown in Fig. 2, the variation of T_{fco} along with time is under 0.1 Nm, which is ignorable. The variation of B is also negligible as well, as shown in Fig. 3.

Next, we attempted to figure out the relationship between δT_f and T_c. Inserting Eq. (8) into Eq. (7) yields,

$$J\frac{d\omega_r}{dt}+B\omega_r=T_e-T_{fco}-\delta T_f-T_c \quad (11)$$

In Eq. (11), since J, B, T_e, T_{fco} and ω_r are either already known or can be measured, Eq. (11) represents the relationship between δT_f and T_c. T_c can be determined at a given ω_r either when the relationship between δT_f and T_c is discovered or when δT_f is a function of given parameters such as J, B, T_e, T_{fco} and ω_r. In this study, the relationship between δT_f and T_c at a given ω_r was determined experimentally. The cutting conditions were varied : 9 different cutting velocities (500～1000 rpm with a step of 100 rpm and 1200, 1400, 1500 rpm) and 6 different depths of cut (0.5～3 mm with an increase of 0.5 mm each set). A commercially available Si_3N_4 ceramic inserts were used to turn AISI1045 workpiece with a diameter of 105 mm, and a tool dynamometer was used for the cutting toque measurement. The results are given in Fig. 4. In Fig. 4, one could easily see that δT_f can be represented as a parabola function of T_c as follows.

$$\delta T_f=C*T_c+D*T_c^2 \quad (12)$$

The coefficients, C and D in Eq. (12) can be obtained by fitting the data measured at the same cutting velocity in the parabola equation. The coefficients C and D are a function of the cutting velocity again, as shown in Figs. 5 and 6. The coefficient C is fitted in the 3rd order difference curve, and the coefficient D is fitted in the parabolic curve as a function of cutting velocity as in Eq. (13).

$$C=C(\omega_r)=-0.54269+0.02318\omega_r-1.96254E-4\omega_r^2+5.64549E-7\omega_r^3 \quad (13)$$
$$D=D(\omega_r)=0.01061-0.00026\omega_r+0.53E-6\omega_r^2$$

C and D are functions of ω_r in Eq. (13). Inserting Eq. (12) into Eq. (11) and rearranging Eq. (11) yield,

$$T_c+C*T_c+D*T_c^2=T_e-B\omega_r-T_{fco} \quad (14)$$

Eq. (14) is a 2nd order difference equation of T_c. Since B and T_{fco} are coefficients and C and D can be calculated from Eq. (13) at a given

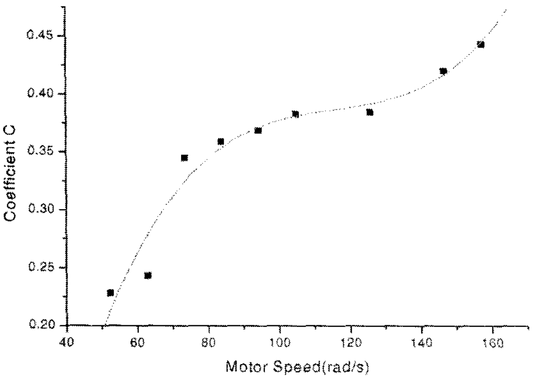

Fig. 5 Curve fitting of coefficient C

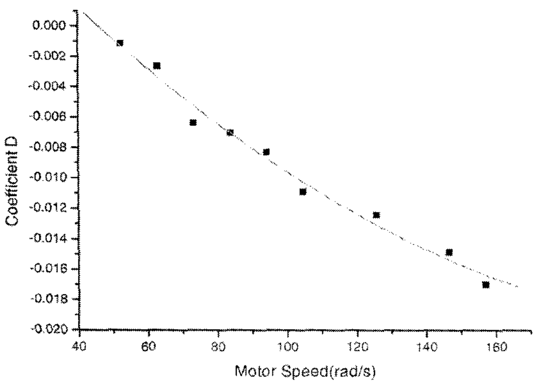

Fig. 6 Curve fitting of coefficient D

angular velocity ω_r, Eq. (14) can be solved regarding T_c at a given cutting velocity.

3. Experimental Setup

For the experiments, we used the Hyundai HiT-15 CNC lathe, whose spindle motor was 1PH6137-4NZ00 of SIEMENS Co. Specifications of the motor is given in Table 1. To measure the cutting force, Kistler 9257B tool dynamometer and 5019A charge amplifier were used. Three-phase stator currents of the induction spindle motor were measured by the 9275 Clamp on AC sensor of HOIKI. Both the currents and the cutting force signal were digitized by the NI-DAQ PCI-MIO16E4 board and stored in a 586pc for the following calculations. These analog signals were also stored in a tape data recorder for the further analysis. A graphical programming was used to construct the torque monitoring system

Table 1 Specifications of induction motor

Phase/Pole	3 phase/4 pole
Rated Power	11 [kw]
Rated Current	41.8 [A]
Rated Speed	750 [m/min.]
Rated Voltage	217 [V]
Rated Frequency	26.3 [Hz]

that could be monitored through the internet. The torque monitoring scheme using the internet is shown in Fig. 7. A web publishing tool provided by LabVIEW was used for a real time monitoring of the torque during machining on CNC lathe. The torque observed and the velocity monitored at a client computer through the internet is shown in Fig. 8.

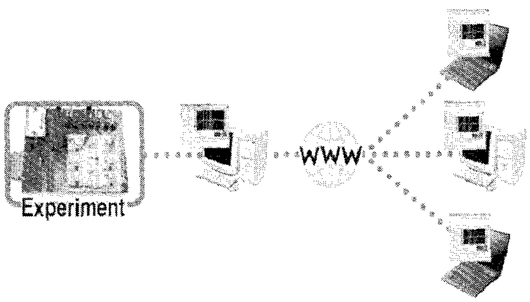

Fig. 7 Torque monitoring of CNC lathe through the internet

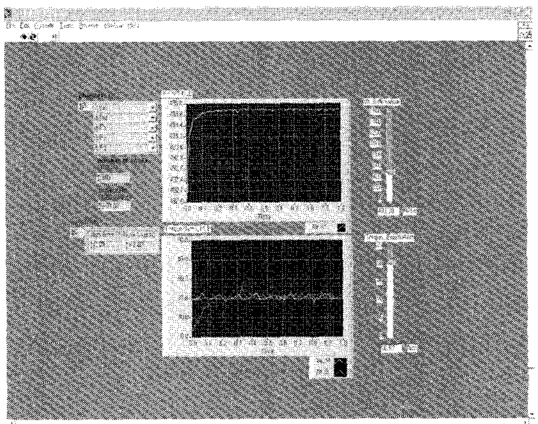

Fig. 8 Torque and velocity monitored at client computer through the internet

4. Results and Discussions

Experiments were carried out under 500, 900, 1000, 1100 and 1500 rpm cutting velocities. Commercially available Si_3N_4 ceramic inserts were used for the experiments with 0.2 mm/rev. feed rate and the depths of cut, 0.5, 1.0, 1.5, and 2.0 mm. 100 data per second per channel were digitized and stored in a personal computer. To reduce the sensitivity of the current signal to the noise, we used the moving average method, in which the average of 20 data was taken. Whenever 1 set of new digitized data was imported to the computer, 1 set of the oldest data was discarded, and the new average values were calculated for a new torque estimation.

In the experiment under the 500 rpm cutting speed and the 1 mm depth of cut, the error of the estimated cutting torque was 2.6% in Fig. 9.

Figure 10 shows the results from machining a workpiece with steps to determine the estimation capability under varying cutting conditions. The depth of each step was 0.5 mm, and the velocity was 500 rpm. Time delay between the reference and the estimated cutting torque was about 0.3 sec when a step was introduced during machining. The result obtained under the cutting condition of 1000 rpm and the 2 mm depth of cut is shown in Fig. 11. The error is 2.8% in this case. In Figs. 12~14, the depth of cut varies from 0.5 mm to 1mm during machining, while the cutting speed is 900 rpm, 1100 rpm and 1500 rpm, respectively. Fig. 12 shows the results under the condition that was not used to obtain the equivalent damping ratio B and the Coulomb frictional force T_{fco}. The cutting condition in Fig. 14 was used neither for the calculation of equivalent damping ratio B and the Coulomb frictional force, T_{fco} nor for the calculation of the increment of the frictional force, δT_f. The errors were different in each step, but the average of the errors was 2.9%. The result acquired at the relatively fast velocity, 1500 rpm, is shown in Fig. 14. The average error in this case is also below 3%.

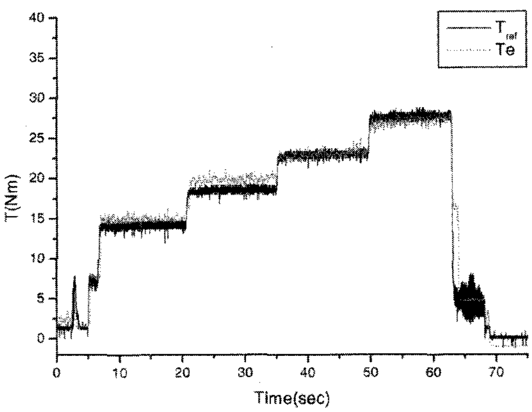

Fig. 10 Estimated and reference cutting torque (Material : AISI1045, Spindle speed : 500 rpm, Depth of cut : 0.5 mm, 1 mm, 1.5 mm, 2 mm)

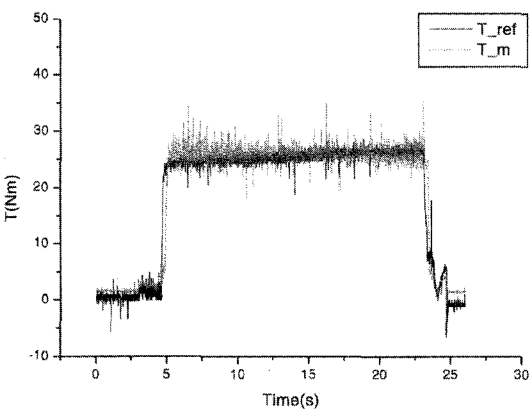

Fig. 9 Estimated and reference cutting torque (Material : Gray cast iron, Spindle speed : 500 rpm, Depth of cut :1 mm)

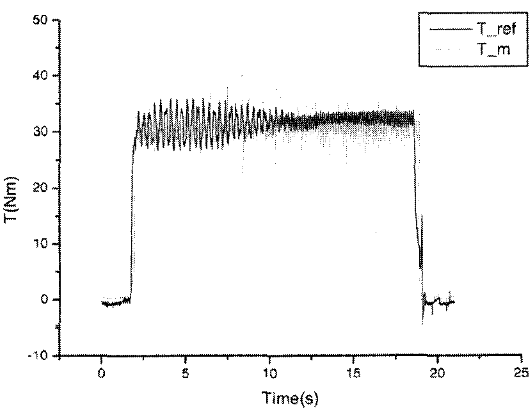

Fig. 11 Estimated and reference cutting torque (Material : AISI1045, Spindle speed : 1000 rpm, Depth of cut : 2 mm)

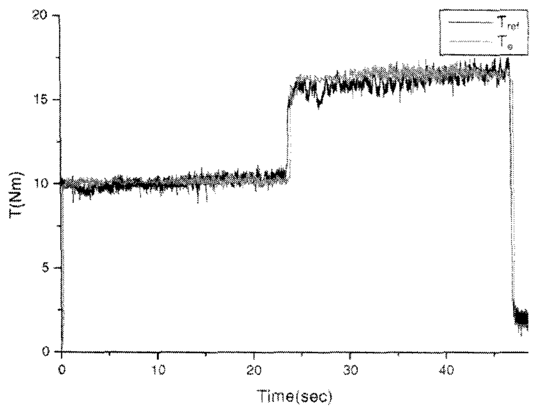

Fig. 12 Estimated and reference cutting torque (Material : AISI1045, Spindle speed : 900 rpm, Depth of cut : 0.5 mm, 1 mm)

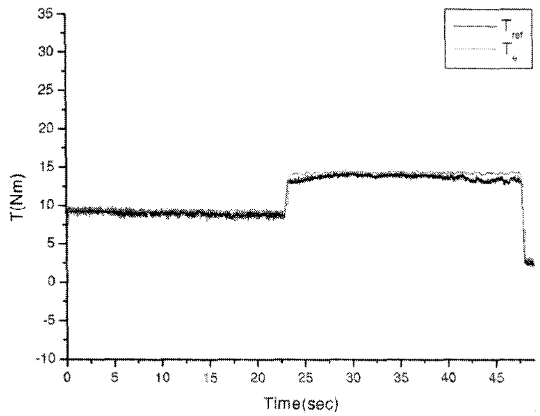

Fig. 13 Estimated and reference cutting torque (Material : AISI1045, Spindle speed : 1100 rpm, Depth of cut : 0.5 mm, 1 mm)

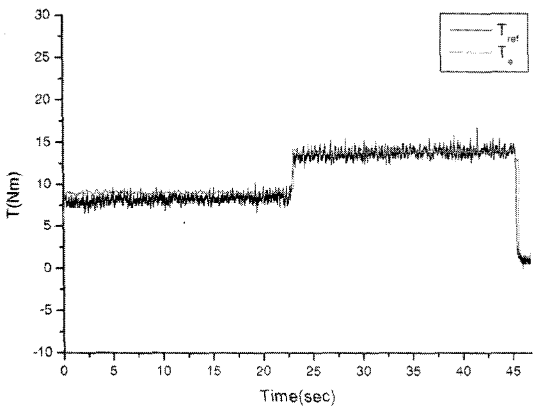

Fig. 14 Estimated and reference cutting torque (Material : AISI1045, Spindle speed : 1500 rpm, Depth of cut : 0.5 mm, 1 mm)

Relatively big errors of 5.3% and 5.8% were occurred in two cases ; one was at the velocity of 1100 rpm and the depth of cut, 1.0 mm, and the other was at the velocity of 1500 rpm and the depth of cut, 2.0 mm. The errors were big because 1100 rpm was not used for the coefficient estimation (as mentioned in chapter 2.2, 9 different cutting velocities (500～1000 rpm with a step of 100 rpm and 1200, 1400, 1500 rpm) and 6 different depths of cut (0.5～3 mm with an increase of 0.5 mm each set) were used for the estimation).

5. Conclusions

The CNC spindle system was divided into two parts for the analysis : electrical part and mechanical part. To increase the accuracy of the estimated torque during machining on the CNC lathe, Coulomb friction and equivalent damping ratio were determined before and after 1000 rpm. On the basis of the measurement of both, increment of the frictional force was also determined as a function of cutting torque and cutting velocity. When the proposed algorithm was applied to the actual system, the average of the error was below 3% under a steady state condition, and the delayed time was 0.3 sec in the transient state. The algorithm proposed in this study was implemented to a computer to monitor the cutting torque using the internet, which showed the satisfactory results.

Acknowledgments

This work was supported by a 2004 research grant from the University of Seoul.

References

Choi, Y. J., 1997, "A Study on Cutting Force Estimation using Spindle Motor Power," M. D. Thesis, Seoul National Univ., Seoul, Korea, in Korea.

Chung, D. H., 1993, "Speed Sensorless Vector Control of Induction Motor for High Performance Control," *Jour. of Institute of Electronics Engineers of Korea*, Vol. 30-B, pp. 1085～1094, in Korea.

Huh, K., Lee, K. and Kim, J., 1999, "Development of a Cutting Force Monitoring System for a CNC Lathe," *Jour. of KSPE*, Vol. 16, No. 1, pp. 219~225.

Lee, K., Jung, J., Kim, J., Huh, K. and Kim, J., 1998, "Development of a Cutting Force Monitoring System for a CNC Lathe," *Jour. of the KSPE Spring Conference*, pp. 440~444.

Mannan, M. A., Broms, S., 1989, "Monitoring and Adaptive Control of Cutting Process by means of Motor Power and Current Measurement," *Annals of CIRP*, Vol. 38, pp. 347~350.

Park, J. J. and Luca, S., 1994, "Cutting Torque Estimation using Spindle Power Measurement," *Trans. of NAMRI/SME*, Vol. 24, pp. 85~90.

Stein, J. L., Colvin, D., Clever, G. and Wang, C. H., 1986, "Evaluation of DC Servo Machine Tool Feed Drives as Force Sensors," *ASME J. of Dynamic Sys. Meas. and Cont.*, Vol. 108, pp. 279~288.